Extended Abstracts of the 2019 International Conference on Solid State Devices and Materials, Nagoya, 2019, pp751-752

Positive Shifting of Threshold Voltage of Nano-Channel (NC) AlGaN/GaN HEMTs with Post Gate Annealing (PGA) Modulation

Soumen Mazumder[1] and Yeong- Her Wang[1*]

[1] Institute of Microelectronics, Department of Electronic Engineering, National Cheng-Kung University, Tainan 701, Taiwan
Phone : +886-6-2757575-62352 E-mail : yhw@ee.ncku.edu.tw

Abstract

A systematic positive shifting of V_{th} of the nano-channel (NC) GaN HEMTs with thinner channel width (W_{NC}) by post gate annealing (PGA) modulation at 400 ^{0}C, is reported. NC-HEMT with different channel width exhibits higher maximum drain current (I_{dmax}), improved gate controllability, higher on off ratio (I_{on}/I_{off}) and lower gate leakage current (I_g).

***Index Terms* — GaN, Nano-channel HEMT (NC-HEMT), Post gate annealing (PGA), threshold voltage (V_{th}).**

1. Introduction

In the rapid growth of communication for high frequency applications, III-V based materials e.g. AlGaN/GaN, high electron mobility transistors (HEMTs) are very useful due to their unique features. For safety and power saving concerns, it is indispensable for HEMT to have a normally off operation. Including quite a few approaches e.g. ion implantation [1], recessed gate [2] etc., nano-channel (NC) HEMT [3] also has a great potential to fabricate E-mode AlGaN/GaN HEMTs. With NC structures E-mode can be achieved with a channel width less than 100 nm, as previously reported [4]. However, since side walls are too close to each other, the transport quality of 2-dimensional electron gas (2DEG) is tainted and I_{dmax} is limited.

Here, we demonstrated an excellent tri-gate controllability on 2DEG channel with post gate annealing (PGA) effect for different NC width (W_{NC}>100 nm) experiences a positive shifting of *threshold voltage* (V_{th}) with higher $I_{dmax,}$ G_{max} and lower gate leakage current (I_g).

2. Experiment

The AlGaN/GaN hetrostructure was composed of a 5.5-µm buffer layer, a 200-nm undoped GaN layer, a 25-nm $Al_{0.23}Ga_{0.77}N$ layer with 1-nm AlN as barrier layer between AlGaN and GaN channel and a 2-nm GaN cap layer. First, an ICP etcher was used to obtain mesa isolation. After that, source and drain regions were defined by photolithography and Ti/Al/Ni/Au were deposited by electron-beam evaporator, followed by RTA at 875 ℃ for 30 s. Then the NC array regions were defined by e-beam lithography having the different channel width (W_{NC} =800, 400, 200 nm) and to form the periodic trench ICP-RIE was carried out with trench depth 100 nm. Finally, the gate region was defined and Ni/Au stack was deposited by e-beam evaporator followed by PGA at 400 ℃ for 10 min. Fig. 1(a) shows the AlGaN/GaN NC-HEMT. As a reference, a conventional HEMT (c-HEMT) was also fabricated. Effective gate widths (W_g) of c-HEMT and NC-HEMTs are 100 and 45 µm respectively having same gate length (L_g =1 µm). A typical AFM image of 200 nm mesa width is shown in Fig.1[(b)-(d)].

3. Result & Discussions

To investigate post gate annealing (PGA) effect on c-HEMT and NC-HEMT, all devices were fabricated without gate annealing at 400 ℃. Maximum drain current (I_{dmax}) has been drastically improved with PGA treatment for both c-HEMT and NC-HEMT with different mesa width. Fig. 2(a) refers the enhancement of I_{dmax} at V_g= 3V achieved to 781, 625, 461 mA/mm [751 mA/mm (c-HEMT)] with PGA treatment, from 770, 541, 388 mA/mm [715 mA/mm (c-HEMT)] for NC-HEMT with channel width 800 nm, 400 nm and 200 nm respectively. Fig. 2(b) demonstrates good I_d-V_d characteristics, particularly showing much reduction of knee voltages as well as ON resistances with PGA for NC-HEMT than conventional one. For NC-HEMT, due to higher effective field (E), I_d becomes larger with lower V_{knee} as well as the reduction of surface states after PGA leads to decrease in $R_{ON.}$

To understand gate controllability of NC-HEMT we also calibrate the transfer and subthreshold characteristics. The transfer characteristics of NC-HEMT and c-HEMT (V_D=3V) are shown in Fig. 3. With decreasing the channel widths (W_{NC}= 200 nm) an organized shift of threshold voltage towards positive (V_{th} = -0.8 V) is observed in NC-HEMT than c-HEMT (V_{th}= -3.4 V). Greater depletion region due to decrease in channel width as well as reduction of strain relaxation induced piezoelectric polarization results the positive shifting of V_{th} in NC-HEMT [4]. Observation confirms from Fig. 3[(a)–(b)], after gate annealing due to better gate controllability V_{th} sifted towards more positive and transconductance (G_m) increases significantly than without PGA. For c-HEMT and NC-HEMT (W_{NC}), G_{max} after annealing is found 150 mS/mm (conventional), 161 mS/mm (800 nm), 147 mS/mm (400 nm) and 138 mS/mm (200nm).

The comparison of subthreshold swing (SS) of c-HEMT and NC-HEMT at V_d = 3V with and without PGA modulation is shown in Fig. 4. The gate leakage characteristics also plotted in Fig. 5. Clearly it has been found that leakage current (I_g) for NC-HEMT (W_{NC}) with PGA is 9.7×10^{-6} mA/mm (800nm), 8.5×10^{-6} mA/mm (400nm), 3.7×10^{-6} mA/mm (200nm) decreases more than three to

four order than without PGA, whereas for c-HEMT I_g decreases only about one order. AFM images suggest that after annealing, the reduction of surface roughness as well as trap states in nano channel force to decrease I_g markedly. In the NC-HEMT the improvement of SS value is found due to the better gate control after PGA. In particular, for NC-HEMT (W_{NC}) with thinner channel width, the SS values are little higher e.g. 96 mV/dec (200 nm), 99 mV/dec (400 nm) due to the ICP etching damage with respect to wider one, as 82 mV/dec (800 nm). Current ratio (I_{ON}/I_{OFF}) also noticeably improved with PGA. For NC-HEMT I_{ON}/I_{OFF} ratio (> 10^8) is much higher than for c-HEMT (~ 10^6). One of the possible reasons for this increment might be the fin structure, by which channel can be controlled from three sides.

4. Conclusions

Threshold voltages of the nano-channel HEMTs (NC-HEMTs) exhibit a systematic shifting towards positive gate voltage (V_g) with thinner channel width (W_{NC}). The decrement of surface states increases channel mobility with PGA modulation, as a result performance of NC-HEMT is even better as I_g, SS as well as R_{ON} reduced markedly while I_{dmax}, I_{ON}/I_{OFF} and G_{max} increased certainly.

Acknowledgements

This study was supported by the Ministry of Science and Technology (MOST), Taiwan, under contract no. MOST 105-2221-E-006-193-MY3.

References

[1] K J. Chen and C. Zhou, Phys. Status Solidi A, 208 (2011) 434.

[2] T.-E. Hsieh, E. Y. Chang, Y.-Z. Song, Y.-C. Lin, H.-C. Wang, S.-C. Liu, S. Salahuddin, and C. C. Hu, IEEE Electron Device Lett., 35 (2014) 732.

[3] S. Liu, Y. Cai, G. Gu, J. Wang, C. Zeng, W. Shi, Z. Feng, H. Qin, Z. Cheng, K. Chen, and B. Zhang, IEEE Electron Device Lett. 33 (2012) 354.

[4] Ohi K, Asubar J T, Nishiguchi K, Hashizume T, IEEE Trans. Electron Devices 60 (2013) 2997.

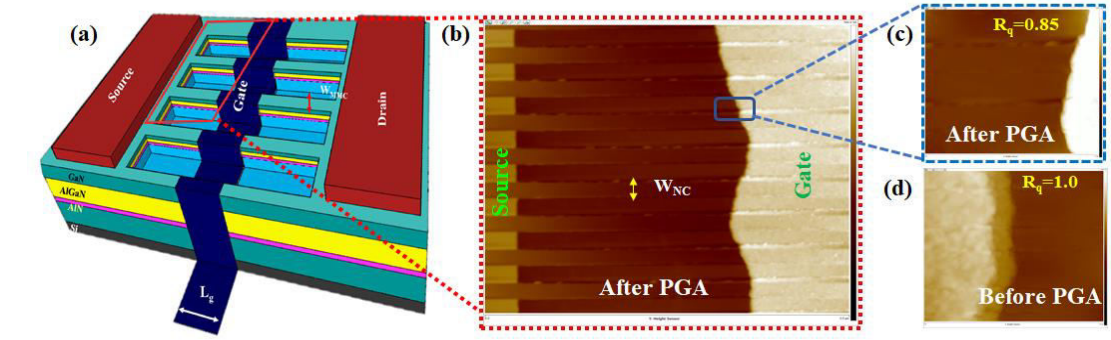

Fig. 1. (a) Schematic illustration of NC-HEMT. (b) AFM image of the GaN surface after the formation of trench with W_{NC} = 200 nm. (c) AFM profile of the channel after PGA & (d) before PGA.

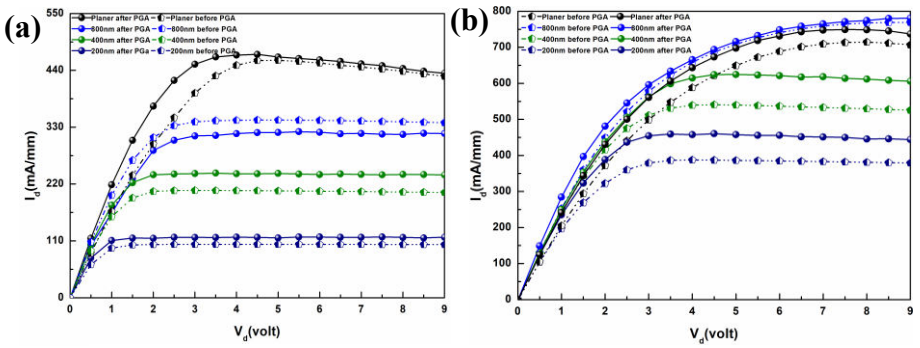

Fig. 2. (a) Comparison of I_{ds}-V_d (V_g = 0V) & (b) I_{dmax}- V_d (V_g= 3V) characteristics for c-HEMT and NC-HEMT with and without PGA at 400 ^{0}C.

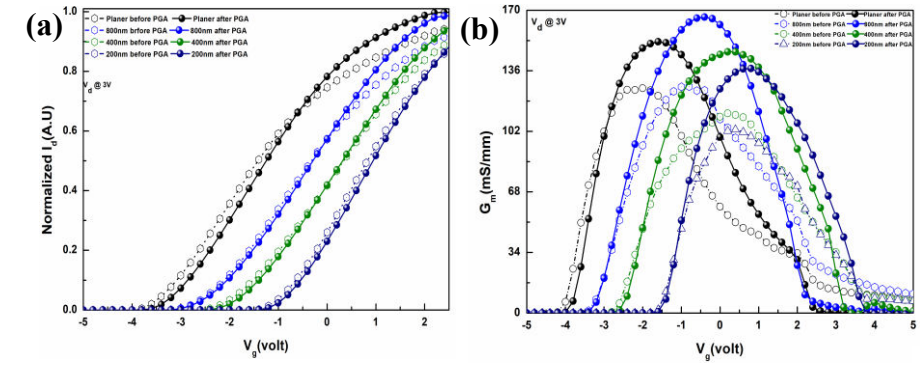

Fig. 3. (a) Comparison of I_d-V_g (V_d = 3V) & (b) Transconductance characteristics for c-HEMT and NC-HEMT before and after PGA.

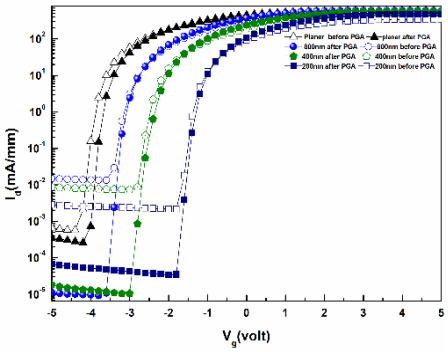

Fig. 4. Subthreshold characteristics (V_d = 3V) for NC-HEMT compared to c-HEMT with and w/o PGA.

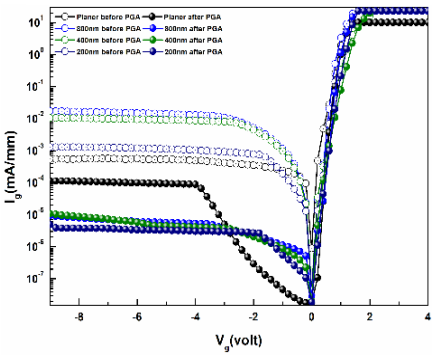

Fig. 5. Before and after PGA effect comparison of leakage current for c-HEMT and NC-HEMT.